ELSEVIER

Journal of Photochemistry and Photobiology A: Chemistry 148 (2002) 25–31

Journal of Photochemistry and Photobiology A:Chemistry

www.elsevier.com/locate/jphotochem

Photoconductivity and charge trapping in porous nanocrystalline titanium dioxide

Jenny Nelson*, Anuradha M. Eppler, Ian M. Ballard

Centre for Electronic Materials and Devices, Department of Physics, Imperial College of Science Technology and Medicine, London SW7 2BZ, UK

Received 13 August 2001; received in revised form 27 November 2001; accepted 27 November 2001

Abstract

We have measured the photoconductivity of symmetrically contacted nanocrystalline anatase TiO_2 films in different chemical environments. The photocurrent can be attributed to the conduction band electron density and can be described quantitatively by a rate equation model which incorporates trapping, recombination and scavenging. In ambient air and in an acetonitrile solvent, the photocurrent is controlled by a competition between two electron loss processes, probably electron–hole recombination and electron scavenging by surface adsorbed species. In vacuum, electron scavenging is suppressed, leading to photocurrents which are increased by a factor of 10^5–10^6 compared to ambient air. This is attributed to the removal of molecular oxygen. Addition of methanol to acetonitrile similarly appears to extend the electron lifetime and leads to much larger photocurrents. This is attributed to the hole scavenging effect of methanol. At low light intensities, in conditions where electron loss processes are suppressed, trap filling effects may be observed. If the photogeneration rate is known, the density of trap states may be deduced. For films in vacuum, the density of effective electron traps is estimated to be less than 10^{20} cm^{-3}. The method is applicable to dye sensitised solar cells, for instance in the evaluation of different hole transporting media, and to photocatalysis.

Keywords: TiO_2; Photoconductivity; Light; Solar cells; Photocatalysis; Trap states

1. Introduction

Porous nanocrystalline TiO_2 is a material of growing technological importance. Films are the basis of dye sensitised solar cells [1], and find applications in electrochromics [2], photocatalysis [3] and biosensors.

The function of devices based on nano-porous TiO_2 depends upon a combination of electron transfer and electron transport steps. Interfacial electron transfer reactions are important because of the very large surface area of the porous film and are the basis of many applications. In addition, charge transport is important for electronic devices such as solar cells. Recent studies of dye sensitised devices have revealed that electron trapping in the nanocrystalline film is the factor which limits the rate of charge recombination between electrons and photo-oxidised dyes, and may limit device performance [4,5]. It is likely that such electron trapping processes influence the behaviour of other devices.

A variety of techniques have been used to probe charge transport in nanocrystalline TiO_2 including current–voltage measurements [6], frequency resolved [7,8] and time resolved [9,10] photocurrent measurements, microwave conductivity [11] and transient absorption [5,12,13]. Most studies have been carried out on devices where asymmetry of the contacts is a complicating factor. In this paper we use photoconductivity as a probe of photogeneration and transport. Photoconductivity reflects the free carrier density and is straightforward to interpret in terms of competition between photogeneration, recombination and trapping, without consideration of spatial variations or sample geometry. As we show below, the signatures of different electron loss mechanisms are easily recognised. We analyse our results with a simple rate equation model based on known electron scavenging mechanisms. We extract information on the density of charge traps and recombination mechanisms under different conditions, which are relevant for application to electronic devices and photocatalysis.

2. Experimental

Colloidal anatase TiO_2 particles of ∼15 nm diameter were prepared as described previously [14]. Porous films were prepared by depositing the colloidal paste on TEC-8 fluorine-doped SnO_2-coated conducting glass and sintering

* Corresponding author. Tel.: +44-20-7594-7581; fax: +44-20-7594-7580.
E-mail address: jenny.nelson@ic.ac.uk (J. Nelson).

1010-6030/02/$ – see front matter
PII: S1010-6030(02)00035-7

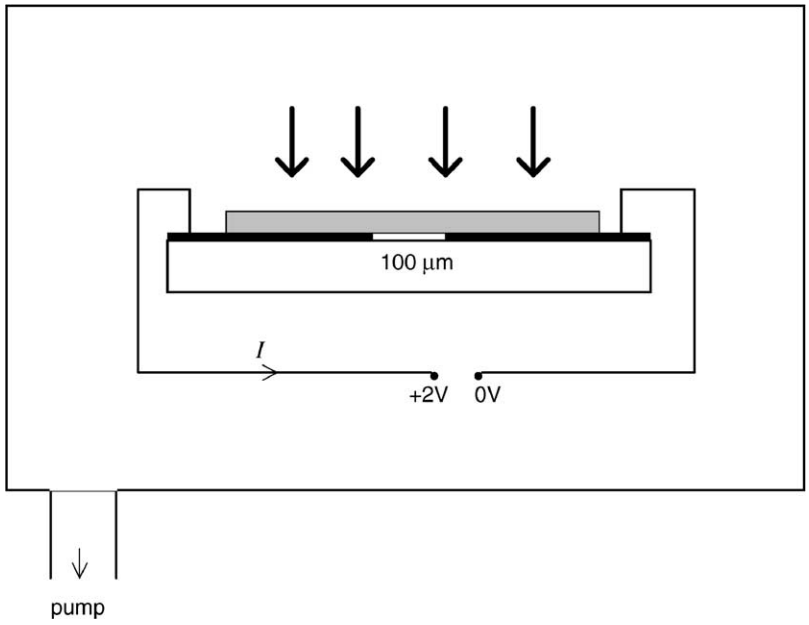

Fig. 1. Schematic of device structure for photoconductivity measurements in air and vacuum.

at 450 °C in air for 10 min. The glass substrates had previously been etched using a diamond saw or by laser ablation to remove a 100 μm strip of the conducting coating. All films reported here were approximately 8 μm thick and 1 cm wide, leaving a bridge of cross-sectional area 1 cm × 8 μm and length 100 μm as the relevant volume for conductivity. The device structure is illustrated in Fig. 1. Qualitatively similar results were obtained on different samples and for samples with an evaporated top contact of titanium and gold.

Electrical measurements were made with Keithley Instruments 238 Source Measure Unit. A Photon Technology International 75 W xenon lamp was used as the light source and directed on to the sample with a liquid light guide. A range of neutral density filters were used to control light intensity, and the intensity was measured with a calibrated silicon photodiode mounted beside the sample. The sample was mounted in an APD Cryogenics vacuum cryostat for measurements in air and vacuum. A rotary pump and diffusion pump were used to reduce the pressure between 10^{-1} and 10^{-6} mbar. Measurements in solvents (99.5% anhydrous acetonitrile and methanol (Aldrich)) were carried out in an electrochemical cell which was modified to allow electrical contacts with the two sides of our sample.

For all experiments a bias of 2 V was applied to the sample, and the current was allowed to stabilise before illumination. The current was recorded as the light was switched on and off for periods between 5 min and 3 h.

3. Results

In the dark, the current (I)–voltage (V) behaviour of the samples follows a power law,

$$I \propto V^{\alpha}$$

where $\alpha > 2$, as expected for space charge limited conduction in the presence of trap states. Current–voltage curves were symmetric, confirming that the contacts are symmetric for charge injection. The resistivity at 2 V was 10^6 to $10^8\ \Omega$ cm in ambient air, rising to 10^9–$10^{10}\ \Omega$ cm in vacuum, and was reproducible between measurements. The conductive behaviour in the dark is the subject of a separate study [15]. For the present purpose, it is sufficient to remark that, for the dry films, dark conductivity is negligible compared to photoconductivity, and that the original dark current value was in all cases eventually recovered after illumination ceased.

In Fig. 2(a) we present the photocurrent as a function of time for a sample measured in ambient air. The figure shows two consecutive periods of illumination separated by a period of darkness. The generation rate in the sample was determined as follows. At a given light intensity the current produced by a calibrated silicon photodiode was recorded, and the spectral photon flux was determined using the emission spectrum of the lamp provided by the manufacturer. The generation rate was calculated from the spectral photon flux using the measured absorbance spectrum of a nominally identical sample of TiO_2. In the case of Fig. 2, the absorbed photon flux was approximately 10^{18} photons $m^{-2}\ s^{-1}$, corresponding to a mean volume photogeneration generation rate of around $10^{24}\ m^{-3}\ s^{-1}$. Two stages can be distinguished in the response to the light: a fast rise over the first few tens of seconds to a maximum, followed by a slower decay over the next few hundred seconds to stabilise at a value of around 20 nA. The response to darkness occurs over a few seconds.

Fig. 2(b) shows the response of the same sample to the same light intensity in a vacuum of around 0.1 mbar. The

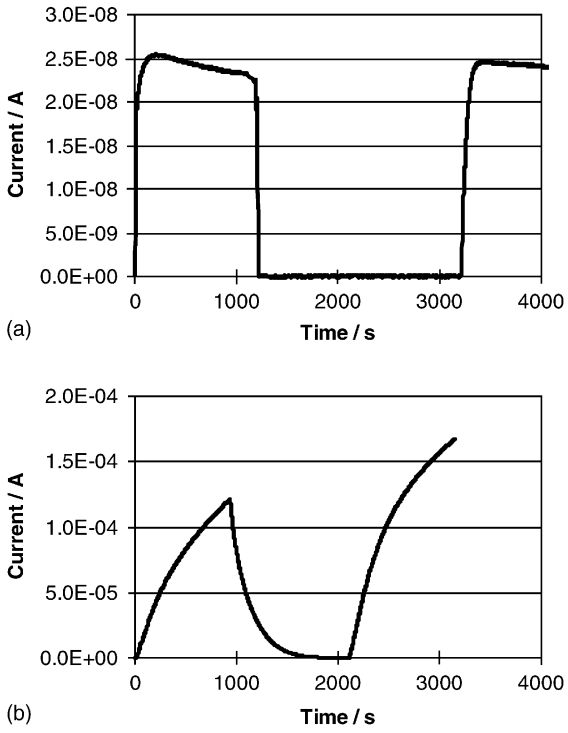

Fig. 2. Photocurrent for a nanocrystalline TiO_2 film illuminated at full intensity (a) in ambient air and (b) in a vacuum of approximately 0.1 mbar. In each case the light was switched off after about 1000 seconds and on again after a period of 1000–2000 seconds in darkness, The times at which the light was switched are clearly marked by the changes in photoconductivity.

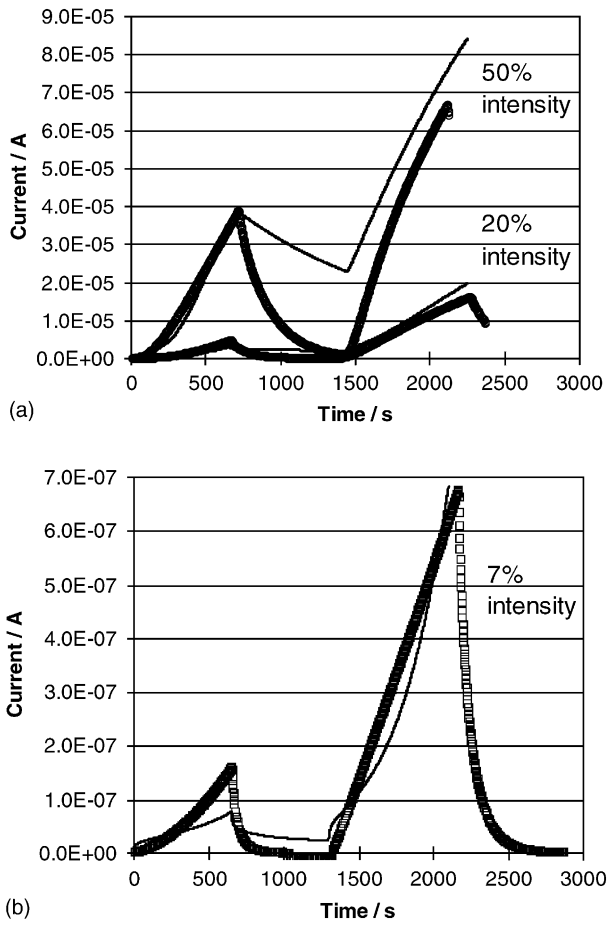

Fig. 3. Photocurrent in vacuum of 0.1 mbar at different light intensities. (a) At approximately 50% and 20% of full intensity; (b) at approximately 7% of full intensity. The full lines are the modelled photocurrents, using the same parameters as Fig. 5(a) and correspondingly reduced light intensities. Notice how the curvature of both data and modelled curves changes as intensity is reduced.

difference is remarkable. First, notice that the photocurrent rises to much higher values. At this light intensity the photocurrent eventually approached a saturation level of around 1 mA after several hours—around 5 orders of magnitude higher than in ambient air. Other important features are the presence of a small point of inflection near the initial rise of the photocurrent, and the faster rise of the photocurrent during the second period of illumination.

In Fig. 3 we present current transients in ambient air for the same sample as Fig. 2 with different light intensities. It is clear that as light intensity is reduced, the point of inflection is moved to longer times and the asymmetry in behaviour between the first and second period of illumination is accentuated. Both these features can be attributed to the filling of traps, as explained below.

The effects of pressure and temperature were studied in the case of the film in vacuum. Reducing the pressure to around 10^{-6} mbar increases the magnitude of the saturation current level by a factor of 2–3, and slows down the rate of recovery in the dark by an order of magnitude. Changing the temperature within a margin of 50 °C around room temperature has a negligible effect, which cannot be distinguished from sample to sample variation. This indicates that the decay is not due to thermal emission of carriers from traps.

Finally in Fig. 4 we present the results for illumination in the presence of a solvent: 99.5% anhydrous acetonitrile (a) and acetonitrile containing around 5% methanol (b). Behaviour in acetonitrile is qualitatively similar to behaviour in air, although reaching much higher current levels. In acetonitrile with methanol, the behaviour resembles that in vacuum. In both cases the dark conductivity is higher. This may be due to current leakage through the solvent, and ease of conduction within the film due to solvation of the surface. The response of the film mounted in the electrochemical cell before any solvent was added was similar to that obtained in ambient air.

It should be stressed that we are confident that we are measuring photoconductivity and not photocurrent generation, because the current under illumination scales linearly with bias over a wide range and vanishes at zero bias. Moreover, the symmetry of the contacts is not expected to support photocurrent generation. In this respect our measurement is distinct from transient photocurrent studies carried out on asymmetric devices [16].

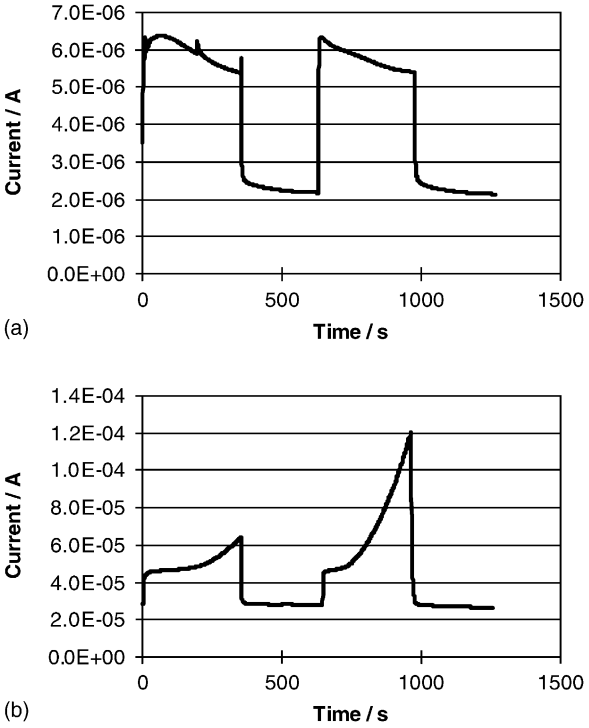

Fig. 4. Photocurrent in different solvents: (a) dry acetonitrile and (b) after addition of approximately 5% methanol. The light intensity was the same as in Fig. 2.

4. Model

We seek a physical model which is capable of explaining the above results. First we assert that the measured current is a measure of the *photoconductivity* of the sample resulting from the photogeneration of free charge carriers. That is, it is not due to photocurrent generation within the sample. In addition, we assume that *electrons* are the dominant charge carrying species in TiO_2 on the basis that photogenerated holes are expected to be trapped at the surface of nanocrystalline TiO_2, and the observation that electrons have much higher mobilities [17]. Under these conditions, the photocurrent reflects the competition between photogeneration and removal of electrons under photogeneration.

From our results, we may make the following observations:

(i) In all cases studied, at least two types of charge carrier removal are in operation. This is deduced from the observation of two time scales for the photocurrent rise leading to either a point of inflection or a maximum.
(ii) The charge removal processes are slow, and are strongly influenced by the ambient environment and pressure.

The model should therefore include at least two electron removal routes and should allow the influence of ambient conditions on the removal processes.

The response of colloidal TiO_2 to photocarrier generation is well studied for applications in photocatalysis [3,18–20]. It is well known that TiO_2 acts as a catalyst for the photoreduction of oxygen and other oxygen containing species, and that hydroxylated Ti sites at the surface may act as traps for electrons or holes, depending on the oxidation state of the Ti ion [18,19]. In addition we may expect to find hydrated surface sites (where the Ti is influenced by molecularly adsorbed water molecules), Ti sites close to an oxygen deficiency, and surface states due to structural imperfections, all of which give rise to a range of traps and recombination centres.

The following reactions may therefore be expected to occur following the photogeneration of carriers:

$$h\nu \rightarrow \mathrm{e} + \mathrm{h} \quad (1)$$

$$\mathrm{e} + \mathrm{h} \rightarrow h\nu/\mathrm{heat} \quad (2)$$

$$\mathrm{e} \rightarrow \mathrm{e_{trap}} \quad (3)$$

$$\mathrm{e_{trap}} + \mathrm{h} \rightarrow h\nu/\mathrm{heat} \quad (4)$$

$$\mathrm{e} + \mathrm{S} \rightarrow \mathrm{S^-} \quad (5)$$

$$\mathrm{e_{trap}} + \mathrm{S} \rightarrow \mathrm{S^-} \quad (6)$$

$$\mathrm{h} + \mathrm{S^-} \rightarrow \mathrm{S} \quad (7)$$

To these must be added the self-photoreduction of TiO_2 which is possible in an oxygen poor atmosphere [18]:

$$2\mathrm{h} + \mathrm{O^{2-}} \rightarrow \mathrm{O_2} \quad (8)$$

Candidates for the electron trap include hydroxylated surface Ti sites, –Ti(IV)–OH, which are reduced to –Ti(III)–OH [18,19] and for the electron scavenger includes molecularly adsorbed oxygen, $O_{2(ads)}$, which is reduced to the superoxide radical anion, $O_2{}^-$. The distinction here between traps and scavengers is that 'traps' are limited in number, while the 'scavengers' are unlimited within the frames of the experiment. A trap may release charge carriers by thermionic emission, depending on its depth. If the reaction (7) is included, then scavenging and trapping are, in principle, equivalent processes. In our analysis, reaction (7) has negligible effect on the results and so can be ignored.

In our analysis we neglect the reaction, $\mathrm{h} \rightarrow \mathrm{h_{trap}}$. Since hole conduction is ignored, we are not able to distinguish trapped from free holes experimentally, and so it is pointless to distinguish them in the model. Neither do we include reaction (8), nor other reactions involving holes. Although reaction (8) may influence photocurrent by leading to the generation of additional electron traps, our data indicate a clear saturation of traps and therefore suggest that this is not a strong effect.

Given our assumption that the electron conductivity is being measured, we are only concerned with the evolution of conduction band electron density, n_{cb}. We may relate n_{cb} to current via

$$I = qn_{cb}\mu_{cb}FA \quad (9)$$

where q the electronic charge, μ_{cb} the mobility of conduction band electrons, F the electric field and A the cross-sectional area.

Now with knowledge of the generation rate (1) and the rate constants defining the reactions (2)–(7) we can simulate the evolution of the current, $I(t)$. This involves solving the coupled rate equations

$$\frac{dn}{dt} = G - \sigma_n n(N_t - n_t) - B(n - n_0)(p - p_0) - k_n S(n - n_0) + \sigma_n e^{(E_c - E_t)/kT}(N_c - n)n_t \quad (10)$$

for conduction band electrons,

$$\frac{dn_t}{dt} = \sigma_n n(N_t - n_t) - \sigma_n e^{-(E_c - E_t)/kT}(N_c - n)n_t - \sigma_p p n_t + \sigma_p e^{-(E_t - E_v)/kT}(N_v - p)(N_t - n_t) \quad (11)$$

for trapped electrons and

$$\frac{dp}{dt} = G - \sigma_p p n_t - B(n - n_0)(p - p_0) + \sigma_p e^{-(E_t - E_v)/kT}(N_v - p)(N_t - n_t) \quad (12)$$

for holes. In the above, G represents the volume photogeneration rate, B, σ_n, σ_p, k_n the coefficients for band to band recombination, electron trapping, hole trapping and electron scavenging, respectively (reactions (2)–(5)). n_0 and p_0 represent the initial values of conduction band electrons and holes, which are fixed, along with the initial trap population, by the initial value of the Fermi level. E_c, E_v and E_t represent the energies of the conduction band edge, the valence band edge and the trap level, respectively, k the Boltzmann's constant and T the temperature. The terms for carrier detrapping are introduced to ensure that detailed balance is satisfied.

The current is calculated by solving Eqs. (9)–(12). To reduce the number of fitting parameters as far as possible, only one effective band to band recombination parameter is used. In the results presented here we have equated the coefficients for recombination via the trap level (reaction (4)) and via the conduction band (reaction (2)), i.e. we set $\sigma_p = B$, but similar results were obtained using other combinations of the two processes. Parameters σ_n, B, k_n, E_t and N_t are fitting parameters within the bounds of reasonable values. Other parameters are taken as follows: the value of G is estimated from the spectral data and photodiode measurements (values given in Fig. 5); the illumination on–off times from the experimental data; the electron mobility as $5 \times 10^{-10}\,m^2\,V^{-1}\,s^{-1}$ according to Ref. [21]; the sample area is $8 \times 10^{-8}\,m^2$ and the electric field as $2 \times 10^4\,V\,m^{-1}$ according to the experimental details; the band gap as 3.2 eV; and the intrinsic Fermi level as 1.6 eV [22].

It is implicit in this picture that the electron density is completely uniform throughout the film. In practice the photogenerated electron density will be graded due to strong light absorption by the TiO_2, and the photogenerated electrons and holes will tend to separate due to a Dember effect from the difference in electron and hole diffusion coefficients. Preliminary studies indicate that neglecting the first effect will lead to an overestimation of the photocurrent [23], while neglecting the second will underestimate electron lifetime and hence photocurrent.

5. Discussion

In this section we will attempt to explain our results, at least qualitatively, using the model as a tool. Complete details of the model and its implications will be published elsewhere.

First, we consider the photoconductive behaviour in vacuum. The much higher saturation currents reached in vacuum, compared to air, indicate slow rates of electron recombination and/or scavenging. The data can be modelled most simply by including photogeneration, trapping and scavenging. The photogeneration rate is responsible for the photocurrent rise. Trapping is necessary to explain the point of inflection in the rise curve and the asymmetry between the first and second rise. This asymmetry can be attributed to the filling of traps during the first period of illumination, which remain filled or partly filled during darkness. During the second period of illumination, fewer photogenerated electrons are trapped and the population of free carriers rises more quickly. The decay in conductivity during darkness indicates that some electron removal process is active. We have modelled this as a slow scavenging process.

Fig. 5(a) presents the results of modelling the data in Fig. 2(b). Including electron trapping does indeed lead to a point of inflection and an asymmetry in the rise curves. Different curves are presented, representing the results for a single trap at different depths. It is clear that neither a single deep nor a single shallow trap can reproduce the observed rise and fall behaviour correctly. Better behaviour is achieved by using an exponential distribution of trap states, of the form,

$$g(E) = \frac{\alpha N_t}{kT} \exp\left(-\frac{\alpha(E_c - E)}{kT}\right) \quad (13)$$

where α is a constant between 0 and 1. Such a distribution of trap states has been invoked elsewhere to explain the charge transport behaviour in nanocrystalline TiO_2 [22,24]. This requires solving multiple rate equations of the form (11) for the different energy intervals in the trap distribution, but introduces only one additional parameter. Using this distribution, with $\alpha = 0.2$, we obtain reasonable agreement with the data but the dark decay is not reproduced exactly. One possible explanation is that electron removal processes accelerate in the dark, but simulating this would introduce further complexity into the model, and is not pursued here.

In ambient air, we expect the rate of scavenging to be increased on account of the greater availability of oxygen. To simulate this we increase S by a factor of 10^4, which is the approximate difference in pressure between the case of air and vacuum in Fig. 2. If all other parameters are left unchanged, we obtain the 'square wave' behaviour represented in Fig. 5(b) by the black line. The good agreement shows

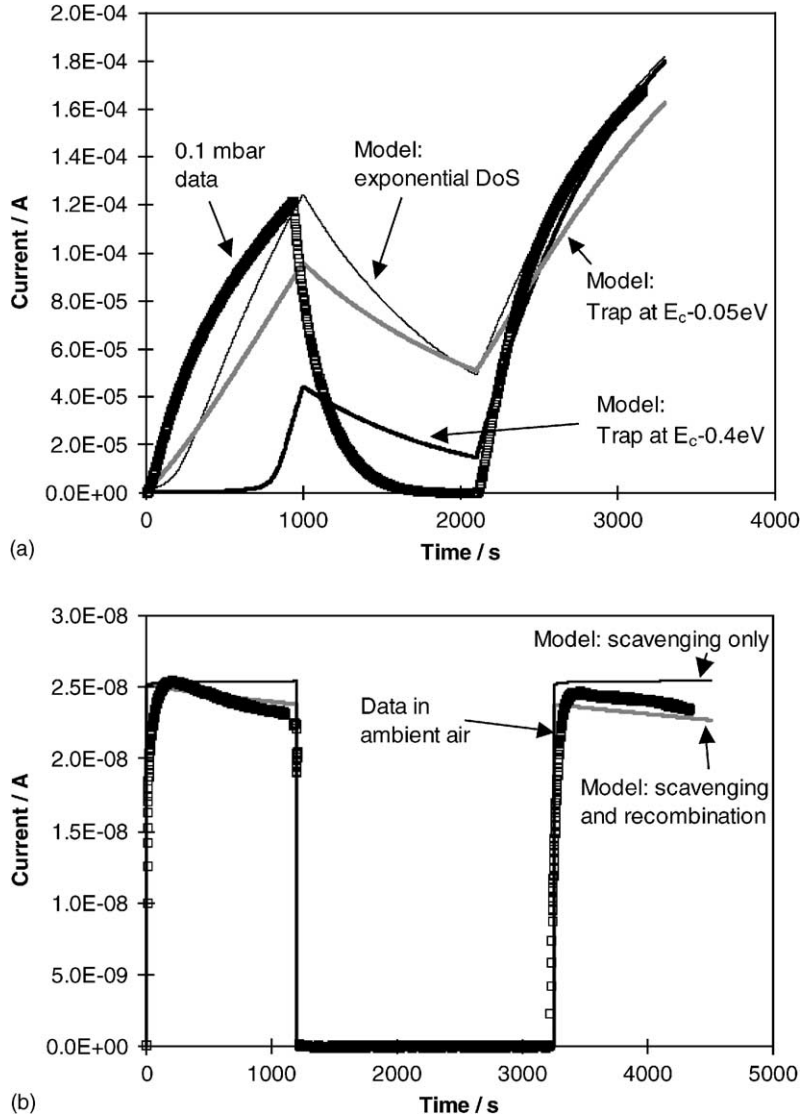

Fig. 5. Modelled photocurrents for the data in Fig. 2, in comparison with the data (open squares). (a) Simulated photocurrent in vacuum. The parameters used are: $G = 10^{24}\,\mathrm{m^{-3}\,s^{-1}}$, $\sigma_n = 1 \times 10^{-27}\,\mathrm{m^3\,s^{-1}}$, $k_n S = 5 \times 10^{-3}\,\mathrm{s^{-1}}$, $\sigma_p = B = 0$ and $N_t = 8 \times 10^{26}\,\mathrm{m^{-3}}$. The full grey line and thin black line are the results for a trap located at a single level 0.4 eV below the conduction band edge, and 0.05 eV below the conduction band edge, respectively. The thick black line is the result for an exponential distribution of traps, according to Eq. (13), with $\alpha = 0.2$. For the distribution, the *effective* density of traps at room temperature is around 10–20% of N_t, on account of thermionic emission. (b) Simulated photocurrent in air. The full black line is the case where only scavenging is included, such that $k_n S = 50\,\mathrm{s^{-1}}$ and $B = 0$. The full grey line is the case where both scavenging and recombination are included, such that $k_n S = 50\,\mathrm{s^{-1}}$ and $B = 1 \times 10^{-27}\,\mathrm{m^3\,s^{-1}}$. All other parameters are as for (a).

that the effect of ambient pressure on photoconductivity can be explained by a removal rate which is proportional to the concentration of scavenging species (probably oxygen) in the ambient. Better agreement with the data is achieved by introducing recombination with holes such that the two loss processes compete, leading to a maximum in the free electron density as observed (grey line). This maximum is due to the competition between recombination, which is non-linear and accelerates with time, and scavenging which is approximately linear.

Now we consider the case of low intensity illumination in vacuum. We have shown that trapping is the primary electron removal process in vacuum at short times. The total amount of charge trapped is determined by the trap density. Therefore, if the light intensity is decreased, trapping effects should be observed over a longer time period, and the point of inflection is moved to longer times, as observed. We have simulated the effect of reducing light intensity by reducing the value of G, and keeping all other parameters as for Fig. 5(a). The results are shown in Fig. 3 together with the data. As expected, reducing G does indeed lead to the observed changes in shape of the curves.

Since the value of G is known and electron removal processes are not dominant in these conditions, the low intensity data gives us a method of determining the density of effective trap states. For this system, we obtain an upper limit of

10^{20} cm^{-3} effective electron traps corresponding to several hundred per nanoparticle.

Finally we comment on the behaviour observed in the presence of solvents. The behaviour in acetonitrile is qualitatively similar to that in air, and can again be modelled as a competition between recombination and scavenging. The electron mobility needed to fit the data appears to be higher in acetonitrile than in air, and the reasons for this are as yet unclear, although it may be related to this due to the effect on surface states of solvation. Introducing methanol is expected to remove photogenerated holes, and this can be simulated most easily by reducing B. We have used the model to simulate the behaviour in both solvents, and find that the effect of methanol can indeed be reproduced by setting $B = 0$ and reducing the scavenging rate. Simulated results are not presented here, as this system is not so well studied and the values of the parameters used need to be checked against other experiments. Nevertheless, we may remark that the model is capable of describing the gross features of the photoconductive behaviour of TiO_2 in solvent as well as gaseous ambients.

6. Conclusions

We have measured the photoconductivity of symmetrically contacted nanocrystalline anatase TiO_2 films in different chemical environments. The photocurrent can be attributed to the conduction band electron density and can be described quantitatively by a rate equation model which incorporates trapping, recombination and scavenging. In ambient air and in acetonitrile, the photocurrent is controlled by a competition between two electron loss processes, probably electron–hole recombination and electron scavenging by surface adsorbed species. Evacuation appears to suppress the electron scavenging and leads to greatly increased photocurrents. This is attributed to the removal of molecular oxygen. Similarly, addition of methanol, which is known to be a hole scavenger, to acetonitrile solvent appears to extend the electron lifetime and leads to much larger photocurrents. At low intensities, in conditions where electron loss processes are suppressed, trap filling effects may be observed, and the density of trap states may be deduced. For films in vacuum, the density of effective electron traps is estimated to be less than 10^{20} cm^{-3}.

The method has relevance to device applications of nanocrystalline TiO_2. A particular application is to dye sensitised solar cells, where photoconductivity can be used to evaluate different chemical environments, such as potential hole transporting materials, in terms of their ability to promote or suppress electron recombination. Another potential application is in chemical sensing. The very large changes in photoconductivity (up to six orders of magnitude in the present work) which appear to result from the presence of oxygen leave scope for photoconductive detection of electron scavenging species by such TiO_2 films.

Studies are currently in progress on the photoconductive behaviour of nanocrystalline TiO_2 in more controlled chemical environments, and in the presence of sensitiser dyes. We are extending the model to include a more detailed description of trapping and reaction kinetics, and to allow for spatial variations and electrostatic effects. Complementary measurements of electron lifetime using transient absorption spectroscopy are in progress. With these improvements we hope to develop a model which can help to predict device performance on the basis of simple photoconductivity measurements. We conclude that photoconductivity appears to be a useful probe of electron availability in TiO_2 films and provides insight into both photocatalytic and photo-electrical processes.

Acknowledgements

We would like to thank Dr. Thierry Lutz and Richard Willis for providing the TiO_2 colloids, Guillaume Maire for help with theoretical model and Dr. James Durrant for useful discussions. We are grateful to the EPSRC and Greenpeace Environmental Trust for funding.

References

[1] B. O'Regan, M. Grätzel, Nature 353 (1991) 737–740.
[2] C. Bechinger, et al., Nature 383 (1996) 608–610.
[3] M.R. Hoffmann, S.T. Martin, W. Choi, D.W. Bahnemann, Chem. Rev. 95 (1995) 69.
[4] S.A. Haque, et al., J. Phys. Chem. B 104 (2000) 538–547.
[5] J. Nelson, et al., Phy. Rev. B 63 (2001) 205321.
[6] S. Sodergren, et al., J. Phys. Chem. 98 (1994) 5552–5556.
[7] P.E. De Jongh, D. Vanmaekelbergh, Phys. Rev. Lett. 77 (1996) 3427–3430.
[8] G. Schlichthorl, N.G. Park, A.J. Frank, J. Phys. Chem. B 103 (1999) 782–791.
[9] A. Solbrand, et al., J. Phys. Chem. B 103 (1999) 1078–1083.
[10] R. Konenkamp, R. Henninger, Appl. Phys. A 58 (1994) 87–90.
[11] J.S. Salafsky, et al., J. Phys. Chem. B 102 (1998) 766–769.
[12] G. Franco, et al., J. Phys. Chem. B 103 (1999) 692–698.
[13] A. Hagfeldt, S.E. Lindquist, M. Gratzel, Sol. Energ. Mat. Sol. C. 32 (1994) 245–257.
[14] C.J. Barbe, et al., J. Am. Ceram. Soc. 80 (1997) 3157–3171.
[15] A.M. Biswas, I.M. Ballard, J. Nelson, Physica E, in press.
[16] K. Schwarzburg, F. Willig, Appl. Phys. Lett. 58 (1991) 2520–2522.
[17] V.Y. Timoshenko, V. Duzhko, T. Dittrich, Phys. Status Solidi (a) 182 (2000) 227–232.
[18] S.H. Szczepankiewicz, A.J. Colussi, M.R. Hoffmann, J. Phys. Chem. B 104 (2000) 9842–9850.
[19] E. Konstantinova, J. Weidmannand, T. Dittrich, J. Porous Mater. 7 (2000) 389–392.
[20] A. Yamakata et al., J. Phys. Chem. B, 2001, in press.
[21] T. Dittrich, E.A. Lebedev, J. Weidmann, Phys. Status Solidi (a) 165 (1998) R5–R6.
[22] R. Konenkamp, Phys. Rev. B 61 (2000) 11057–11064.
[23] G. Maire, Final-year Project, Department of Physics, Imperial College, London, 2001.
[24] J. Nelson, Phys. Rev. B 59 (1999) 15374–15380.